

# WHAT CAN WE LEARN FROM COMPARISON BETWEEN CUPRATES AND HE FILMS? : PHASE SEPARATION AND FLUCTUATING SUPERFLUIDITY

Y. J. UEMURA

Dept. of Physics, Columbia University, New York, NY 10027, U.S.A.

E-mail: tom o@kirby.phys.columbia.edu

In the underdoped, overdoped, Zn-doped or stripe-forming regions of high- $T_c$  cuprate superconductors (HTSC), the superfluid density  $n_s = n$  at  $T = 0$  shows universal correlations with  $T_c$ . Similar strong correlations exist between 2-dimensional superfluid density and superfluid transition temperature in thin films of  $^4\text{He}$  in non-porous or porous media, and  $^4\text{He}/^3\text{He}$  film adsorbed on porous media. Based on analogy between HTSC and  $^4\text{He}$  film systems, we propose a model for cuprates where: (1) the overdoped region is characterized by a phase separation similar to  $^4\text{He}/^3\text{He}$ ; and (2) pair (boson) formation and fluctuating superconductivity occur at separate temperatures above  $T_c$  in the underdoped region.

The magnetic field penetration depth of superconductors is related to the superconducting carrier density  $n_s$  divided by the effective mass  $m^*$ , as  $1/\lambda^2 \propto n_s/m^*$ . In this paper, we shall refer to  $n_s = n$  as the "superfluid density". Since the discovery of HTSC, we have performed muon spin relaxation (SR) studies of under- to optimally doped [1,2], overdoped [3], and Zn-doped [4] cuprates, as well as HTSC systems associated with the formation of static spin stripes [5,6]. In all of these systems, we found strong correlations between  $n_s = n$  at  $T = 0$  and  $T_c$ , as shown in Fig. 1. This figure suggests that the superfluid density is likely a crucial determining factor for  $T_c$  of all these HTSC systems. These correlations in the underdoped region have been interpreted in terms of Bose-Einstein (BE) to BCS crossover [7-9], phase fluctuations [10], XY model [11], as well as via RVB-type [12] pictures.

Thin films of  $^4\text{He}$  also exhibit strong correlations between their two-dimensional superfluid area density  $n_{s2d} = n$  and  $T_c$ . In Figure 2, we replot published results of  $^4\text{He}$  film on mylar sheet (non-porous media) [13], vycor glass (porous media) [14,15], as well as thin film  $^4\text{He}/^3\text{He}$  mixture on alumina powder (porous media) [16]. The horizontal axis was obtained after converting the He coverage into 2-dimensional (2-d) areal boson density divided by the boson mass  $n_{b2d} = n_b$ , and then into the 2-d Fermi temperature  $T_{F2d}$  assuming  $n_{b2d} = n_{s2d}/2$  and  $m_b = 2m$ . The Kosterlitz-Thouless (KT) transition temperature  $T_{KT} = T_{F2d}/8$  for the strong coupling limit [17] is shown by the solid line.  $T_c$  scales with  $T_{KT}$ , as expected for an ideal Bose gas composed of tightly-bound fermion pairs in a pure 2-d environment.

Figures 1 and 2 exhibit striking resemblance. In Zn-doped HTSC systems [4], the superfluid density  $n_s = n$  at  $T = 0$  decreases with increasing Zn concentration as shown in Fig. 3(a). To explain this result, we proposed a "swiss cheese model" [4], where each Zn suppresses superconductivity of the surrounding region characterized by the in-plane coherence  $\xi_{ab}$  on the  $\text{CuO}_2$  planes, as illustrated in Fig. 3(d). The solid lines represent the expected superfluid density estimated from the ratio of superconducting versus non-superconducting regions. Without any fitting, this

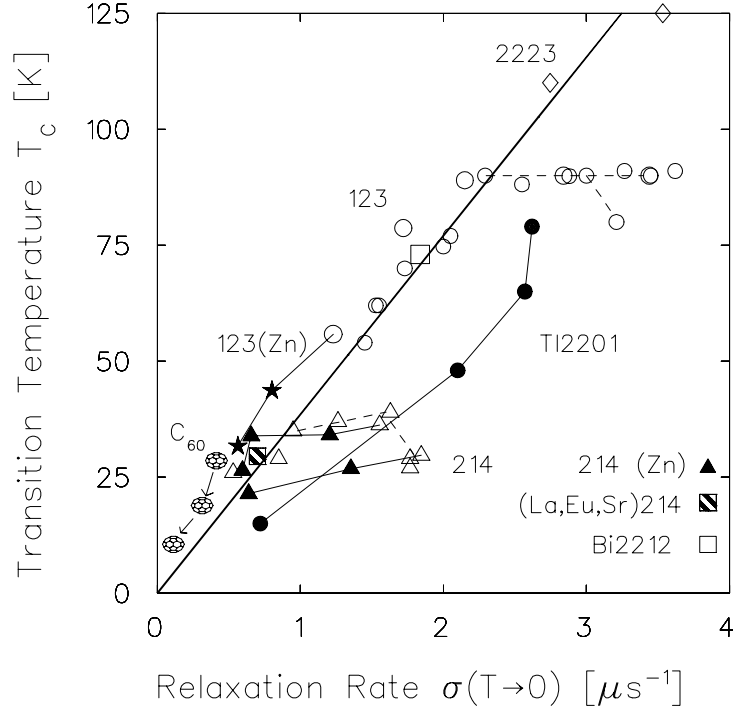


Figure 1. Superconducting transition temperature  $T_c$  of HTSC systems plotted versus muon spin relaxation rate  $(T \rightarrow 0) / 1 = 2 / n_s = m$  [1-5]. Y123 systems on the solid line are in the underdoped region, while Tl2201 systems are in the overdoped region.

model gives a very good agreement with the experimental data. Recently this picture was confirmed directly by the scanning tunnelling microscope studies of Pan et al. [18].

As shown in Fig. 1,  $T_c$  of the Zn-doped cuprates follow the trajectory of hole-doped cuprates without Zn [4]. This suggests that Zn reduces  $n_s = m$ , and the volume average value of  $n_s = m$  then determines  $T_c$ . This situation looks quite analogous to  $^4\text{He}$  films adsorbed on porous media, where a part of He forms a normal layer (i.e. a "healing layer") between the porous substrate and superfluid, while  $T_c$  is determined by the amount of the superfluid portion.

Recently, Kojima et al. [5] found that  $\text{La}_{1.75}\text{Eu}_{0.1}\text{Sr}_{0.15}\text{CuO}_4$  (LESCO) undergoes magnetic order with static stripe freezing occurring in about half of the volume fraction below  $T_N \approx 10$  K. This system becomes superconducting below  $T_c \approx 30$  K. The superfluid density could be determined even below  $T_N$ , thanks to the signal from the remaining non-magnetic volume. The results show that  $n_s = m$  is reduced to about a half of the value for  $\text{La}_{1.85}\text{Sr}_{0.15}\text{CuO}_4$  without stripe formation. This is consistent with a picture where hole carriers in the regions with the frozen static spin stripes do not participate in the superfluid. As shown in Fig. 1,  $T_c$  again scales with the volume averaged value of  $n_s = m$  in LESCO with static stripes. Similar scaling with the trends of other 214 cuprates has been found in the SR results of

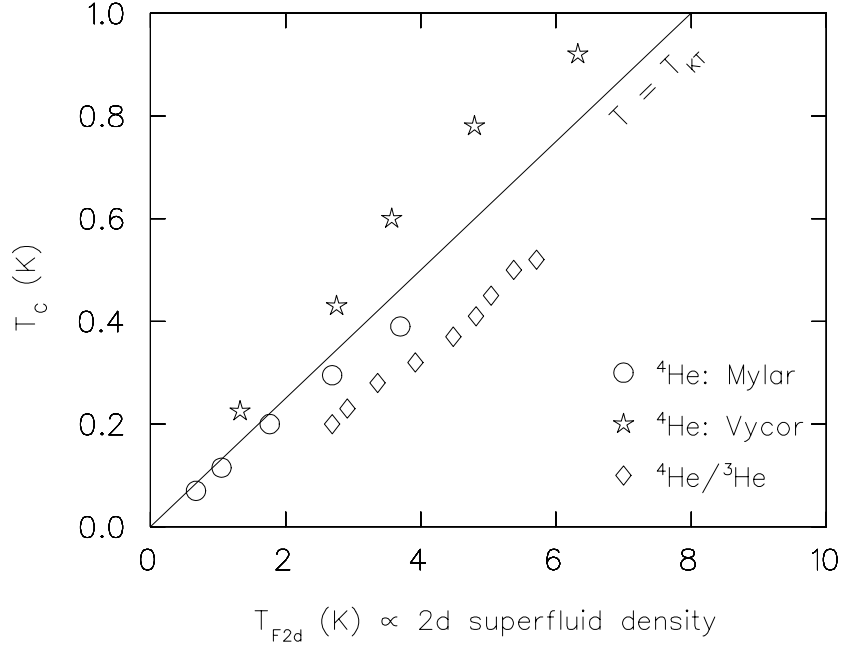


Figure 2. Superfluid transition temperature  $T_c$  of  $^4\text{He}$  film adsorbed on Mylar film [13], porous Vycor glass [14,15] and  $^4\text{He}/^3\text{He}$  mixture adsorbed on fine alumina powder [16], plotted versus 2-d superfluid density at  $T = 0$ . The horizontal axis is shown by converting 2-d boson density  $n_{b2d}$  and mass  $m_b$  into fermionic language as  $n_{b2d} = n_{s2d}/2$  and  $m_b = 2m$  and then calculating the corresponding 2-d Fermi temperature  $T_{F2d} = n_{s2d}/m$ . The solid line indicates the superfluid density expected at the Kosterlitz-Thouless transition temperature  $T_{KT}$ .

$T_c$  versus  $n_s/m$  in single crystals of  $\text{La}_2\text{CuO}_{4.12}$  and  $\text{La}_{1.88}\text{Sr}_{0.12}\text{CuO}_4$  [6], both of which having stripe spin freezing detected in a partial volume fraction of muon sites. The region with frozen stripes, though its size and origin are yet to be clarified, looks analogous to the non-superconducting region around Zn in Zn-doped cuprates.

In overdoped Tl2201, SR studies [3,19] revealed that  $n_s/m$  decreases with increasing hole doping, as shown in Fig. 3(b). Since no signature of anomalous behavior has been found from  $\mu$ , this result suggests that  $n_s$  becomes smaller than the normal state carrier concentration  $n_n$ . Indeed a specific heat study in Tl2201 [20] suggests co-existence of gapped (A) and un-gapped (B) responses, with the latter portion increasing with increasing doping. These results can be explained if we assume a microscopic phase separation between superfluid and non-superconducting fermionic carriers [3,8,9,21], as illustrated in Fig. 3(d).

A mixture of  $^4\text{He}$  and  $^3\text{He}$  provides a typical example of phase separation. With an increasing fermionic portion of  $^3\text{He}$ ,  $T_c$  decreases, maintaining an approximate proportionality to  $p_4^{2/3}$  where  $p_4$  denotes the volume fraction of  $^4\text{He}$ . Thin films of  $^4\text{He}/^3\text{He}$  can be adsorbed on porous media, such as fine alumina powders, which constrain the phase separation to be microscopic. In Fig. 3(c), we show the re-

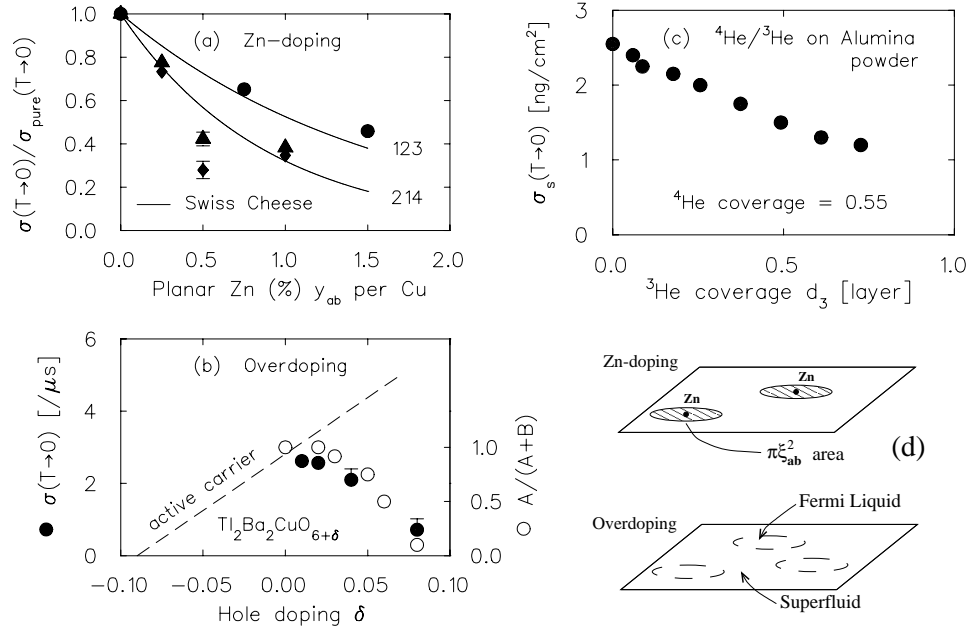


Figure 3. Depletion of the superfluid density due to perturbation: (a) Zn-doping in  $\text{YBa}_2\text{Cu}_3\text{O}_{6.63}$ ,  $\text{La}_{1.85}\text{Sr}_{0.15}\text{CuO}_4$  and  $\text{La}_{1.8}\text{Sr}_{0.2}\text{CuO}_4$  [4]; (b) Overdoping in  $\text{Tl}_2\text{Ba}_2\text{CuO}_{6+\delta}$  [3]; and (c)  $^3\text{He}$  mixing in  $^4\text{He}$  adsorbed on alumina powder [16]. (d) illustrates the Swiss cheese model with Zn doping [4], and proposed phase separation in overdoped HTSC. Open circles in (b) represents the relative weight of the gapped response (A) normalized to the sum of gapped (A) and ungapped (B) responses in the linear-T term of the specific heat measurements by Loram et al. [20].

duction of superfluid density with increasing  $^3\text{He}$  fraction  $p_3$  using the results in ref. [16]. In this case, due to the 2-d configuration,  $T_c$  decreases approximately as  $T_c/p_4 = (1 - p_3)$ . Thus, both in  $^4\text{He}/^3\text{He}$  and in overdoped Tl2201, we see a suppression of the superfluid density and  $T_c$  due to increasing fermionic fraction in a microscopic phase separation.

Based on these analogies, we propose a new phase diagram for HTSC systems in Fig. 4. As stated in our previous publications [7-9,21], we consider the "pseudo-gap" temperature  $T^*$  to represent a signature of pair (boson) formation. In this case,  $T^*$  reflects the magnitude of the attractive interaction between fermionic carriers. If this attractive interaction rapidly decreases with increasing hole doping near the "optimal  $T_c$ " region, there is no robust superconductivity in the overdoped region. However, the system can phase separate into regions with "optimal hole density (OHD)" (corresponding to "optimal  $T_c$ ") which maintain superconductivity and those with higher hole density (HHD) without superconductivity. The charge imbalance will cost extra energy to phase separate while bulk superconductivity could gain condensation energy. The OHD region would correspond to the  $^4\text{He}$ -rich superfluid while HHD region to the  $^3\text{He}$ -rich normal fluid in analogy to  $^4\text{He}/^3\text{He}$ .

Recently Loram, Tallon and co-workers [22] noticed a sharp reduction of the  $T$

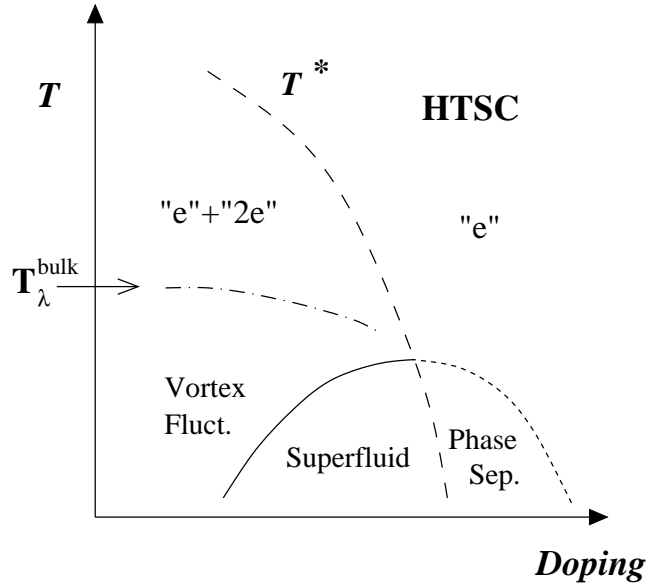


Figure 4. Proposed new phase diagram for HTSC systems. With decreasing temperature in the underdoped side, individual fermion carriers starts forming pairs below  $T^*$ , and time-dependent superconductivity appears below  $T_c$ . In the overdoped side, there is no pairing interaction, and superconductivity survives via phase separation.

line near the hole concentration of  $x = 0.19$  per Cu. They argued that this phenomenon is incompatible with superconductivity observed at  $x = 0.19$  in the overdoped region, if  $T^*$  represents the superconducting pairing interaction. However, our picture with phase separation provides a way to reconcile the sharp reduction of the pairing energy scale  $T^*$  with the survival of superconductivity in the overdoped region.

Signatures of fluctuating superconductivity have been found in the underdoped cuprates above  $T_c$  in studies of high-frequency optical conductivity  $\sigma_{ac}$  [23], the Nernst effect [24], and the "resonance" inelastic scattering intensity in neutron scattering [25]. We notice that all these results show onset of their effect below  $T \sim 150$  K, which is substantially lower than  $T^*$  determined from the c-axis conductivity [26] and/or NMR Knight shift [27]. The analogy to Helium can provide a possible explanation to this feature.

In the case of He, formation of bosons (He atoms) from fermions occurs at very high temperatures. At a much lower temperature  $T_{bulk} = 2.2$  K (the bulk transition point) BE condensation occurs in a 3-d environment. In a highly 2-d environment, the bulk superfluidity occurs at lower temperature  $T_c$ . Time-dependent superfluidity via unbound vortices occurs between  $T_c$  and  $T^*$  in the 2-d situation. Similarly to this, we expect the two step process, i.e., pair formation at a high temperature  $T^*$  followed by signatures of fluctuating superconductivity at much lower temperature below  $T_c$  ( $T_c < T < T^*$ ) for underdoped cuprates, as

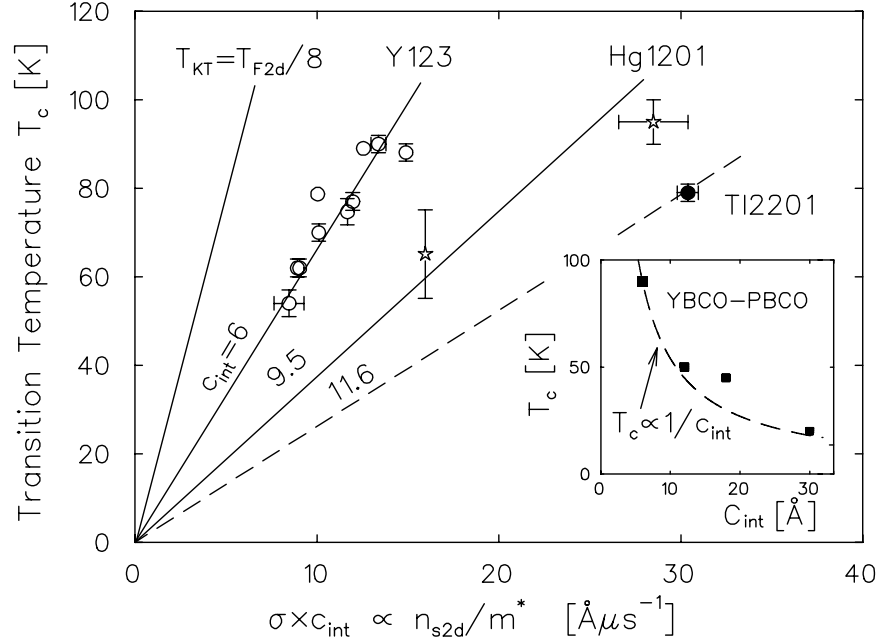


Figure 5. Plot of  $T_c$  versus  $c_{int} / n_{s2d} = m / T_{F2d}$  in underdoped and nearly optimally-doped HTSC [1,3,28] systems.  $T_{KT}$  shows the strong coupling limit in pure 2-d. Inset:  $T_c$  vs.  $c_{int}$  in multilayer YBCO-PBCO films [29].

illustrated in Fig. 4. We can ascribe the  $\rho_{ac}$ , Nernst, and neutron results to the onset of time-dependent superconductivity below  $T^*$  while the c-axis transport and Knight shift to the formation of singlet fermion pairs below  $T_c$ . Formation of a pair (boson) does not immediately correspond to quantum condensation, which requires a certain density/mass to achieve phase coherence of bosonic wave functions.

Despite all these analogous features, there exists an important difference between HTSC and Helms. Figure 5 shows a plot of  $T_c$  versus the 2-d area superfluid density  $n_{s2d} = m$  obtained for cuprates by multiplying  $n_s = m$  with the average distance  $c_{int}$  between the  $\text{CuO}_2$  planes. We notice that: (A)  $T_c$  for the cuprates are 2-4 times reduced from  $T_{KT}$  calculated for the strong-coupling limit; (B) for a given  $n_{s2d} = m$ ,  $T_c$  is higher for systems with smaller  $c_{int}$  (consistent with the results in inset for YBCO-PBCO multilayer films). The feature (B) is incompatible with the KT transition in pure 2-d systems where  $T_c$  should not depend on a 3-d coupling via  $c_{int}$ . Previously, we pointed out that BE condensation in quasi 2-d systems would provide a better account for the observed dependence of  $T_c$  on  $c_{int}$  [9,21].

Finally, we would like to point out that fluctuating superconductivity can be expected not only for the KT transition but also for BE-condensation in quasi 2-d systems. Analogous, for example, to spin fluctuations in quasi 2-d magnetic systems, correlations develop already at the temperature corresponding to the transition temperature  $T_{c3d}$  for a 3-d environment, while long-range order occurs at a much

lower temperature  $T_{c2d}$  due to dimensionality effects. The correlated spin fluctuations at  $T_{c2d} < T < T_{c3d}$  correspond to the fluctuating superfluidity in HTSC and  $^4\text{He}$ . In BE condensation in the quasi 2-d situation,  $T_c$  is determined at a point where thermal energy becomes comparable to the interlayer interaction enhanced by the fluctuating in-plane superconducting correlations. This process is essentially similar to how  $T_c$  for magnetic order is determined in quasi 2-d spin systems. Thus, the  $\mu_{ac}$ , Nernst, and neutron results cannot distinguish between a pure KT transition versus quasi 2-d BE condensation. This point requires further studies.

#### Acknowledgement

The author is grateful to M. Randeria for helpful discussions. This study is supported by NSF (DMR-98-02000) and US-Israeli Binational Science Foundation.

#### References

1. Y. J. Uemura et al., Phys. Rev. Lett. 62 (1989) 2317-2320.
2. Y. J. Uemura et al., Phys. Rev. Lett. 66 (1991) 2665-2668.
3. Y. J. Uemura et al., Nature 364 (1993) 605-607.
4. B. Nachum et al., Phys. Rev. Lett. 77 (1996) 5421-5424.
5. K. M. Kojima et al., submitted to Phys. Rev. Lett. (2000).
6. A. Savici et al., Physica B 289-290 (2000) 338-342; and unpublished
7. Y. J. Uemura, in Proceedings of the Workshop in Polarons and Bipolarons in High- $T_c$  Superconductors and Related Materials, Cambridge, 1994 ed. by E. Salje et al. (Cambridge Univ. Press, 1995) pp. 453-460;
8. Y. J. Uemura, in Proceedings of the CCAST Symposium on High- $T_c$  Superconductivity and the  $C_{60}$  Family, Beijing, 1994 ed. by S. Feng and H. C. Ren (Gordon and Breach, New York, 1995) pp. 113-142.
9. Y. J. Uemura, Physica C 282-287 (1997) 194-197.
10. V. J. Emery and S. Kivelson, Nature 374 (1995) 434-437.
11. T. Schneider, Z. Phys. B 88 (1992) 249-253; T. Schneider and H. Keller, Int. J. Mod. Phys. 8 (1993) 487-528.
12. P. A. Lee and N. Nagaosa, Phys. Rev. B 46 (1992) 5621-5639; P. A. Lee and X. G. Wen, Phys. Rev. Lett. 78 (1997) 4111-4115.
13. G. Agnolet, D. F. M. Cooney and J. D. Reppy, Phys. Rev. B 39 (1989) 8934-8958.
14. D. J. Bishop, J. E. Berthold, J. M. Parpia and J. D. Reppy, Phys. Rev. B 24 (1981) 5047-5057.
15. K. Shirahama, M. Kubota, S. Ogawa, N. Wada, T. Watanabe, Phys. Rev. Lett. 64 (1990) 1541-1544; P. A. Crowell, F. W. Van Keuls, and J. D. Reppy, Phys. Rev. B 55 (1997) 12620-12634.
16. H. Chyo and G. A. Williams, J. Low Temp. Phys. 110 (1998) 533-538.
17. E. Babaev and H. Kleinert, Phys. Rev. B 59 (1999) 12083-12089.
18. S. H. Pan et al., Nature 403 (2000) 746-750.
19. Ch. Niedermayer et al., Phys. Rev. Lett. 71 (1993) 1764-1767.

20. J.W. Loram, K.A. Mirza, J.M. Wade, J.R. Cooper, and W.Y. Liang, *Physica C* 235-240 (1994) 134-137.
21. Y.J. Uemura, invited paper presented at the M2S-HTSC-VI Conference in Houston, Feb., 2000, *Physica C* in press.
22. J.W. Loram, J. Lou, J.R. Cooper, W.Y. Liang and J.L. Tallon, presented at Crest International Workshop, Nagoya, Japan, January, 2000, *J. Phys. Chem. Solids*. in press; and references therein.
23. J. Corson, R. M. Allozzi, J. Orenstein, J.N. Eckstein, I. Bozovic, *Nature* 398 (1999) 221-223.
24. Z.A. Xu, N.P. Ong, Y. Wang, T. Kakeshita and S. Uchida, *Nature* 406 (2000) 486-489.
25. P. Dai, H.A. Mook, G. Aeppli, S.M. Hayden, F. Dogan, *Nature* 406 (2000) 965-968.
26. T. Ito, T. Ido, H. Takagi and S. Uchida, *Nature* 350 (1991) 569-572.
27. See, for example, H. Alloul, T. Ohno, P. Mendels, *Phys. Rev. Lett.* 63 (1989) 1700-1703.
28. B. Nachum et al, *Hyperne Interact.* 105 (1997) 119-124.
29. O. Fischer et al, *Physica B* 169 (1991) 116.